ELSEVIER

Journal of Nuclear Materials 296 (2001) 112–118

journal of nuclear materials

www.elsevier.com/locate/jnucmat

Microstructural origins of radiation-induced changes in mechanical properties of 316 L and 304 L austenitic stainless steels irradiated with mixed spectra of high-energy protons and spallation neutrons

B.H. Sencer [a,b,*], G.M. Bond [a], M.L. Hamilton [b], F.A. Garner [b], S.A. Maloy [c], W.F. Sommer [c]

[a] *New Mexico Institute of Mining and Technology, Socorro, NM 87801, USA*

[b] *Materials Resources Department, Pacific Northwest National Laboratory, P.O. Box 999, Building #326, Battelle Boulevard, P8-15, Richland, WA 99352, USA*

[c] *Los Alamos National Laboratory, Los Alamos, NM 87545, USA*

Abstract

A number of candidate alloys were exposed to a particle flux and spectrum at Los Alamos Neutron Science Center (LANSCE) that closely match the mixed high-energy proton/neutron spectra expected in accelerator production of tritium (APT) window and blanket applications. Austenitic stainless steels 316 L and 304 L are two of these candidate alloys possessing attractive strength and corrosion resistance for APT applications. This paper describes the dose dependence of the irradiation-induced microstructural evolution of SS 316 L and 304 L in the temperature range 30–60°C and consequent changes in mechanical properties. It was observed that the microstructural evolution during irradiation was essentially identical in the two alloys, a behavior mirrored in their changes in mechanical properties. With one expection, it was possible to correlate all changes in mechanical properties with visible microstructural features. A late-term second abrupt decrease in uniform elongation was not associated with visible microstructure, but is postulated to be a consequence of large levels of retained hydrogen measured in the specimens. In spite of large amounts of both helium and hydrogen retained, approaching 1 at.% at the highest exposures, no visible cavities were formed, indicating that the gas atoms were either in solution or in subresolvable clusters. Published by Elsevier Science B.V.

1. Introduction

An understanding of the response of candidate materials to the irradiation conditions they will experience in the accelerator production of tritium (APT) facility is essential to proper development of its components [1]. Very limited information was previously available for application of 300-series steels in such severe environments. Accelerator-driven spallation environments such as APT will produce high radiation damage levels, concurrent with high rates of helium and hydrogen generation, and in APT, at relatively low irradiation temperatures. Irradiation data on these steels that are already available were derived, in general, from situations involving relatively low particle energies, much lower gas (He/H) generation rates, and much lower doses, compared to those expected in APT.

Therefore specimens of APT candidate materials were irradiated at the 800 MeV 100 mA Los Alamos Neutron Science Center (LANSCE) accelerator in off-beam neutron furnaces to relatively low exposures, and to displacement levels as high as ~15 dpa in the direct proton beam in order to simulate various APT conditions [1]. Nevertheless, even the high exposure data

* Corresponding author. Tel.: +1-509 376 0156; fax: +1-509 376 0418.

E-mail address: bulent.sencer@pnl.gov (B.H. Sencer).

0022-3115/01/$ - see front matter. Published by Elsevier Science B.V.
PII: S0022-3115(01)00512-8

obtained will have to be extrapolated to doses 2–3 times higher to predict materials performance under APT conditions for its expected service life. In order to extrapolate the mechanical property data with confidence to higher exposures, a good understanding of the microstructural changes responsible for changes in mechanical behavior is essential.

Changes in tensile properties of the materials irradiated in the mixed proton and spallation neutron spectra at LANSCE have been reported earlier, as shown in Fig. 1 [2,3]. Both 304 L and 316 L stainless steel also exhibit an initial strong hardening at the low (<0.1 dpa) damage levels attained in the neutron furnaces, where the specimens were far away from the proton beam. At the higher in-beam doses the 300-series steels maintain the initial radiation-induced hardening. The uniform elongation of the 300-series steels falls relatively slowly with increasing dose, and then drops precipitously again at doses around 3–4 dpa. Helium and hydrogen measurements on both 316 L and 304 L specimens examined in this study have also been reported [4,5]. The retained helium increases continuously at a rate of ~180 appm dpa^{-1} while the hydrogen retention is higher by about a factor of two, as shown in Fig. 2.

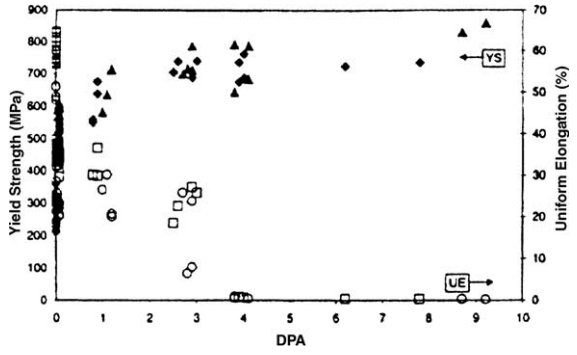

Fig. 1. The yield strength (solid syymbols) and uniform elongation (open symbols) of 304 L (diamond and square symbols) and 316 L (triangular and circular symbols) irradiated at low-temperatures and tested at 20–164°C [3].

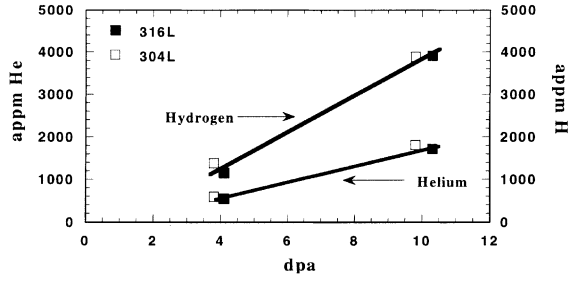

Fig. 2. Measured helium and hydrogen levels in 300 stainless steel vs dpa [4,5].

To investigate the microstructural evolution of the 300-series alloys in a mixed proton and spallation neutron environment, in-beam specimens ranging between 0.7 and 10.3 dpa were examined by transmission electron microscopy (TEM). The present paper describes the radiation-induced microstructural evolution of these alloys and its role in the concurrent changes in mechanical properties.

2. Experimental conditions

316 L and 304 L are with a nominal composition of Fe–17.26%Cr, 12.16%Ni, 2.57%Mo, 0.65%Si, 0.13%Mn, 0.26%Cu, 0.019%C, 0.006%S, 0.022%P, and Fe–18.23%Cr, 9.68%Ni, 0.33%Mo, 0.54%Si, 1.77%Mn, 0.38%Cu, 0.02%C, 0.002%S, 0.026%P, in wt%, respectively. Standard 3 mm diameter microscopy specimens for both steels were electro-discharge-machine (EDM) cut from as-received (annealed) material, and received no further heat treatment prior to irradiation.

The irradiation was conducted in LANSCE facility at Los Alamos National Laboratory. Details of the irradiation were published previously [1]. Doses were determined through analyzing the isotopes produced in activation foils placed alongside specimens [6]. The irradiation temperatures were determined from thermocouples placed in each reference tube [7]. Irradiated specimens were chosen for microstructural evaluation depending on the proton beam intensity at their location.The materials examined, together with the irradiation temperatures and doses, are shown in Fig. 3,

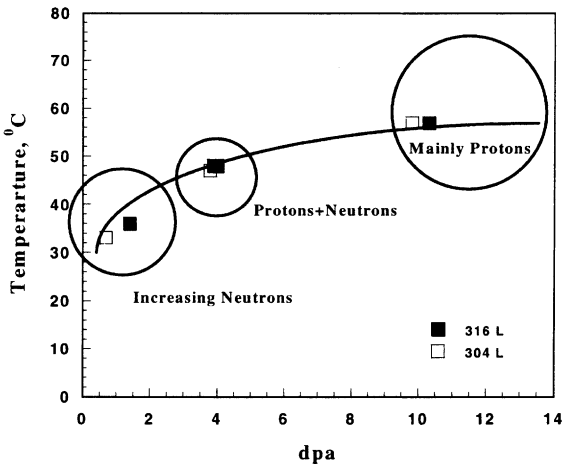

Fig. 3. Description of specimens examined, together with the irradiation temperature, dose and type of energetic particles responsible for radiation damage. At high doses (≥9.6 dpa), the flux is mainly high-energy protons, at medium doses (3–5 dpa) protons and spallation neutrons, and at low doses (<1.4 dpa) increasing spallation neutrons.

which also shows which types of energetic particle were responsible for the radiation damage to the materials.

Thin-foil samples were prepared for TEM examination by conventional jet electropolishing methods, using a 5% perchloric acid, 95% methanol solution at -20°C and 50 V for both steels. TEM examinations were conducted with a JEOL 2000E (200 keV) and a JEOL 1200EX (120 keV) for the diffraction-contrast microstructural characterization.

3. Results

3.1. 316 L /304 L stainless steels

The microstructure of unirradiated annealed 316 L and 304 L contains a very low dislocation density. Proton and spallation neutron irradiation produced a significant change in the general microstructure of both annealed 316 L and 304 L stainless steels. Black-spot damage (BSD) was present at all dpa levels. Fig. 4 shows BSD and larger faulted Frank loops in bright-field (BF), weak-beam dark-field (DF) and relrod images of faulted Frank loops for 316 L at 1.3, 3.9 and 10.3 dpa, respectively. Microstructural evolution of 304 L is shown in BF and in weak-beam DF images in Fig. 5, at 0.7 and 9.8 dpa, respectively. Relrod images of faulted Frank loops are also shown in Fig. 5 for 304 L at 0.7, 3.8, and 9.8 dpa, respectively.

Electron diffraction patterns did not show any precipitate reflections. The possibility of cavity formation was investigated in Fresnel contrast. The technique allows identification of cavities down to a resolution of $\sim$1 nm [8]. However, no cavity (bubble and/or void)

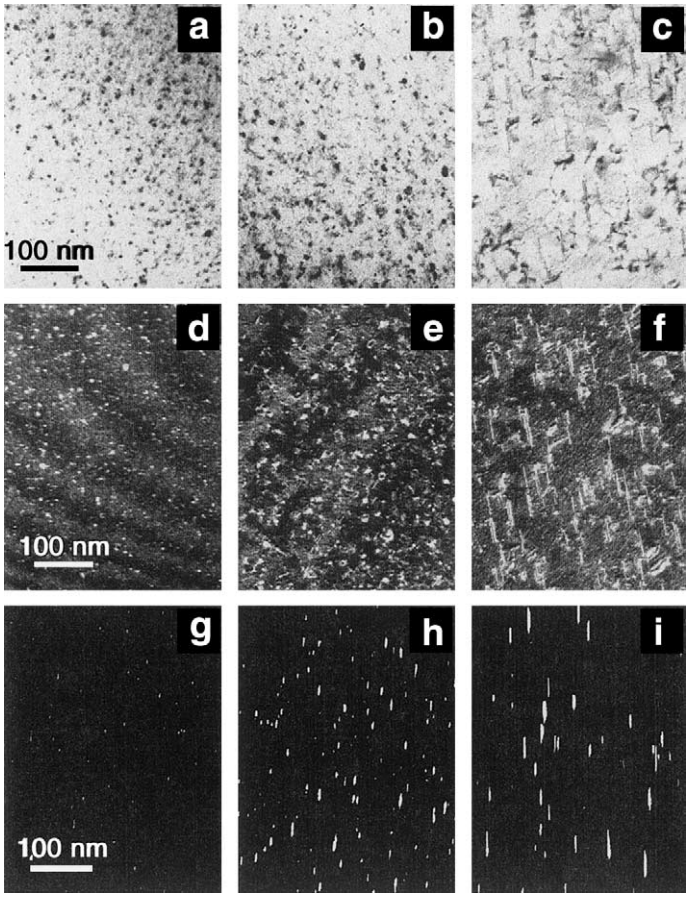

Fig. 4. BF TEM micrographs of 316 L, showing small defect clusters and larger faulted Frank loops, $g = 200$, $s > 0$ at (a) 1.3, (b) 3.9 and (c) 10.3 dpa. Weak-beam DF $g = 200$ ($g/4g$) TEM micrographs of 316 L, showing BSD and larger faulted Frank loops, taken with beam direction close to $\langle 1\,1\,0\rangle$ zone axis, at (d) 1.4, (e) 3.9 and (f) 10.3 dpa. TEM micrographs of 316 L showing faulted Frank loops, taken with beam direction close to $\langle 1\,1\,0\rangle$ zone axis; (g), (h) and (i) are DF images taken from one of the $\langle 1\,1\,1\rangle$ relrods for samples at (g) 1.3, (h) 3.9 and (i) 10.3 dpa.

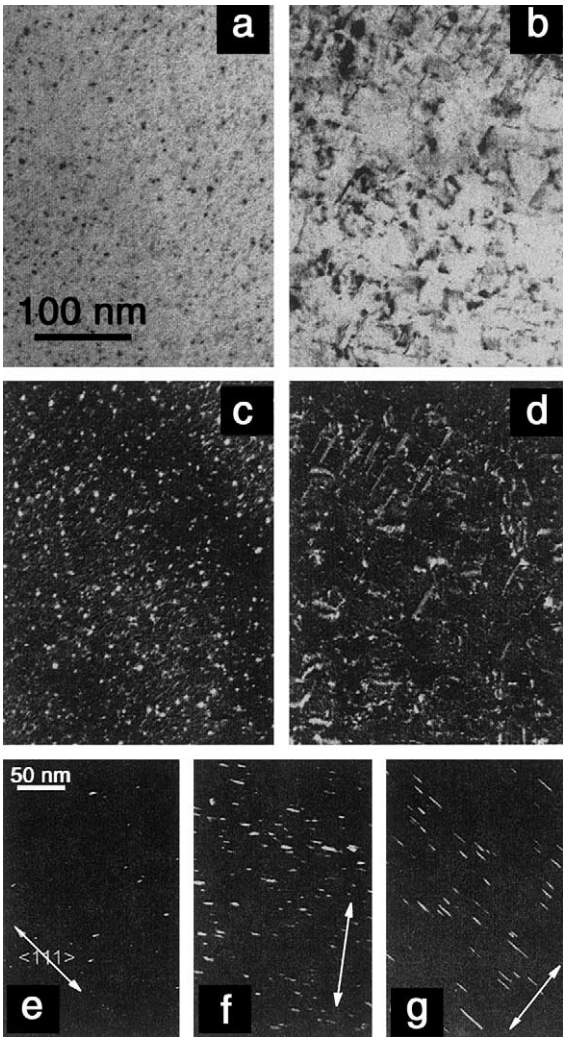

Fig. 5. BF TEM micrographs of 304 L, showing small defect clusters and larger faulted Frank loops, $g = 200$, $s > 0$ at (a) 0.7, and (b) 9.8. Weak-beam DF $g = 200$ $(g/4g)$ TEM micrographs of 304 L, showing small defect clusters and larger Frank loops, taken with beam direction close to $\langle 1\,1\,0\rangle$ zone axis, at (c) 0.7 and (d) 9.8 dpa. TEM micrographs of SS 304 L showing faulted Frank loops, taken with beam direction close to $\langle 1\,1\,0\rangle$ zone axis; (e), (f) and (g) are DF images taken from one of the $\langle 1\,1\,1\rangle$ relrods for samples at 0.7, 3.8, and 9.8 dpa, respectively.

formation was found in the samples irradiated to the higher dose (10.3 dpa).

Fig. 6(a) shows loop size distributions for 304 L at doses of 0.7, 3.8 and 9.8 dpa. Similar distributions were seen for 316 L as shown in Fig. 6(b). Average loop size and the density of loops, as well as the total dislocation density (associated with the loops) of both steels are given in Table 1, and shown in comparison in Figs. 7(a)–(c), respectively.

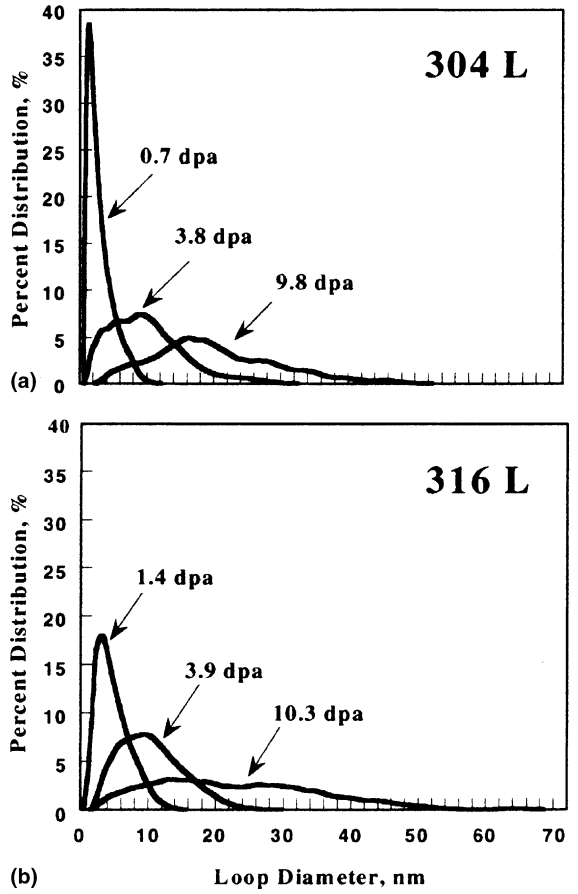

Fig. 6. (a) Loop size distributions for 304 L samples at 0.7, 3.8 and 9.8 dpa; (b) loop size distributions for 316 L samples at 1.4, 3.9 and 10.3 dpa.

4. Discussion

Typical radiation-induced microstructural features in austenitic stainless steels (SS) are dislocation loops, network dislocations, cavities and precipitates. Pronounced changes in microstructural behavior in austenitic stainless steels occur as a function of irradiation temperature. As reported in the literature, the microstructural evolution can be divided into two temperature regimes. In the low-temperature regime (<300°C) of interest to the current study, the microstructure of austenitic stainless steels is dominated by small defect clusters (often referred to as BSD), faulted dislocation loops, and network dislocations [9].

The microstructure of SS 316 irradiated with fusion and fission neutrons at 90°C and 250°C between 0.01 and 0.03 dpa revealed small loops [10]. Radiation-induced precipitation was not observed at either temperature. Comparison of dislocation densities in SS 316 after irradiation at 290°C and at 90°C showed that the

Table 1
Summary of dislocation loop densities, mean loop diameters, and total dislocation densities for irradiated 316 L and 304 L

Material	Dose (dpa)	Loop number density (m^{-3})	Mean loop diameter (nm)	Total dislocation density of loops (m^{-2})
316 L	1.4	2.1×10^{22}	4	2.6×10^{14}
316 L	4.1	4.8×10^{22}	10.2	1.54×10^{15}
316 L	10.3	1.9×10^{22}	23.6	1.41×10^{15}
304 L	0.7	1.6×10^{22}	1.8	9.0×10^{13}
304 L	3.8	5×10^{22}	9.6	1.35×10^{15}
304 L	9.8	2.1×10^{22}	20.1	1.32×10^{15}

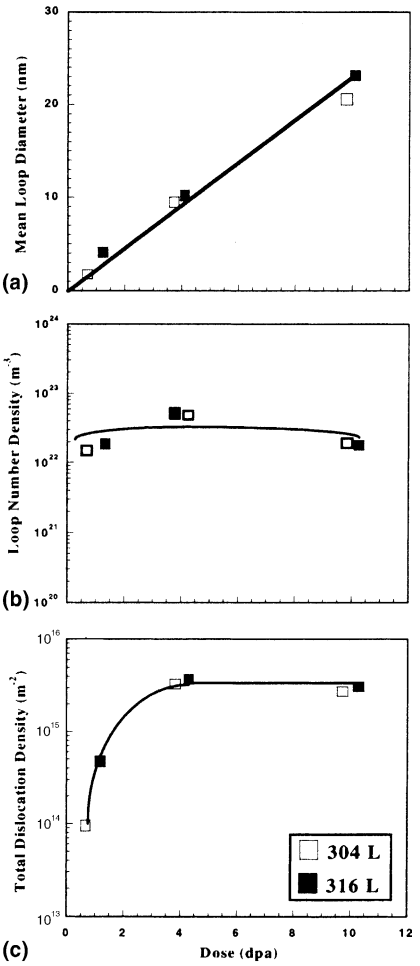

Fig. 7. (a) Mean loop diameter; (b) loop number density; (c) total dislocation density as a function of dpa, for two 300-series stainless steels irradiated with mixed spectra of protons and spallation neutrons.

dislocation density was about 10 times smaller at 90°C. With increasing temperature in low-temperature regime, the density of BSD decreased, and the density of Frank loops and network dislocations increased in cold-worked (CW) stainless steels. Radiation-induced phases are not generally observed in the low-temperature regime [9]. However, HFIR-irradiation at 90°C and 250°C induced the formation of precipitates, which were identified as G-phase ($M_6Ni_6Si_7$) and $M_{22}C_6$ carbides [11]. Carbides were found only in the matrix. Near 300°C, the radiation-induced microstructure changes from BSD to larger faulted loops, network dislocations and cavities. Due to a lack of irradiation studies on stainless steel at very low temperatures (<60°C), the dose dependence of the small defect clusters, network dislocations and faulted dislocation loops, as well as the mechanical properties, is not well established.

Combined proton and spallation neutron irradiation in the current study produced less pronounced, but still significant changes in the microstructure of both 304 L and 316 L in the temperature range of 30–60°C. BSD was present at all dpa levels, while the larger faulted Frank loops became more numerous at higher doses. At 0.7 dpa the predominant microstructural feature is BSD or small Frank loops, reaching 50 nm at 9.8 dpa in 304 L. The average loop diameter at 0.7 dpa is smaller by a factor of 10 than that at 9.8 dpa. Neither electron diffraction patterns nor stereo-micrographs revealed any evidence of radiation-induced precipitation in the matrix or at the grain boundaries.

The microstructures of 316 L and 304 L austenitic stainless steels are remarkably similar after irradiation under similar irradiation conditions. Both materials essentially contain BSD and larger faulted Frank loops. The density of loops increases quickly at very low doses, and changes only a little with inscreasing dose thereafter. At ~4 dpa, the densities of loops in both 316 L and 304 L are identical within the scatter of the data. For both alloys, the overall microstructure coarsens as a function of increasing dose.

The microstructural response of the two steels to the irradiation is so similar that it is not surprising to see similar trends in the mechanical behavior [2,3]. If the observed radiation-induced changes in mechanical properties are to be explained in terms of the microstructural alterations induced by radiation, it is important to check whether the hardening observed in the

300-series stainless steels can be explained in terms of only the microstructural alterations observed. The obstacle strength (α) values required to produce the hardening observed in our current study have been reported earlier [12]. Calculated α (0.3–0.5) values for small loops and black-spots between ~4 and 10.3 dpa are close to the expected values [13]. There were no precipitates or cavities observed in this study; only black-spots and larger Frank loops were formed.

Nothing can be determined from this study about the possible contribution of the accumulating gas atoms to the hardening, but the fact that the Frank-loop hardening contributions saturate, as does the yield strength, tends to argue that the increasing gas (in either atomistic form or subresovable clusters) is not contributing significantly to the hardening. The retained helium increases continuously at a rate of ~180 appm dpa^{-1}, while the hydrogen retention is twice higher [4]. Retention of ~592 appm helium and ~1380 appm hydrogen at ~4 dpa, and ~1812 appm helium and ~3885 appm hydrogen at ~10 dpa was measured, indicating that essentially all of the generated helium and a significant fraction of the generated hydrogen has been retained. It is important to note that, in the current study, the maximum gas retention (helium, hydrogen) was ~0.7 at.%. However, increasing helium above 1 at.% levels, bubbles were formed and grew continuously at 200°C in 316 LN austenitic steel, after 5 at.% helium implantation, bubble lattices were reported [14].

The results of electron microscopy of radiation damage evolution on undeformed specimens have been shown to account for all features observed in radiation-induced evolution of mechanical properties except for the second and most precipitous drop of uniform elongation in 304 L and 316 L stainless steels at ~3 dpa. Initial examination of irradiated and deformed microstructures of both 304 L and 316 L shows that the deformation mode of both steels after irradiation is twinning. No strain induced phase transformation was observed to occur. Therefore, it is proposed that gas accumulation, especially that of hydrogen, may be the cause of this abrupt decrease in uniform elongation.

5. Conclusions

Based on the combined results of mechanical testing, gas retention, and microstructural evolution, the following conclusions can be drawn.

Proton and spallation neutron irradiation induces the formation of both BSD and larger faulted Frank loops in 316 L and 304 L stainless steels. Radiation-induced precipitation did not occur in either steel.

At ~4 dpa, mean loop sizes, loop number densities and total dislocation densities are similar for the two steels, within the scatter of the data. There was no significant difference in the microstructural evolution of 316 L and 304 L under these irradiation conditions.

In spite of the large levels of helium and hydrogen retention, no cavities were found even at the highest dose examined.

The increase in yield stress in both steels is due primarily to formation and evolution of faulted Frank loops, with gas playing no large role.

The loss of ductility observed in both steels is due to a combination of, first, radiation-induced hardening by BSD and larger loops, and second, gas accumulation at higher doses (>3 dpa).

Acknowledgements

This work was supported by the US Department of Energy under the Accelerator Production of Tritium Program At Los Alamos National Laboratory. Battelle Memorial Institute operates Pacific Northwest National Laboratory for USDOE.

References

[1] S.A. Maloy, W.F. Sommer, R.D. Brown, J.E. Roberts, J. Eddleman, E. Zimmerman, G. Willcutt, in: M.S. Wechler, L.K. Mansur, C.L. Snead, W.F. Sommer (Eds.), Proceedings of the Symposium on Materials for Spallation Neutron Sources, TMS, Warrendale, PA, 1998, p. 35.

[2] M.L. Hamilton, F.A. Garner, M.B. Toloczko, S.A. Maloy, W.F. Sommer, M.R. James, P.D. Ferguson, M.R. Louthan Jr., J. Nucl. Mater. 283–287 (2000) 418.

[3] S.A. Maloy, M.R. James, G.J. Willcutt, W.F. Sommer, W.R. Johnson, M.R. Louthan Jr., M.L. Hamilton, F.A. Garner, in: S.T. Rosinski, M.L. Grossbeck, T.R. Allen, A.S. Kumar (Eds.), Effects of Radiation on Materials, 20th International Symposium, ASTM STP 1405, American Society for Testing and Materials, West Conshohocken, PA, 2002, in press.

[4] B.M. Oliver, F.A. Garner, S.A. Maloy, W.F. Sommer, P.D. Ferguson, M.R. James, in: S.T. Rosinski, M.L. Grossbeck, T.R. Allen, A.S. Kumar (Eds.), Effects of Radiation on Materials, 20th International Symposium, ASTM STP 1405, American Society for Testing and Materials, West Conshohocken, PA, 2002, in press.

[5] F.A. Garner, B.M. Oliver, L.R. Greenwood, M.R. James, P.D. Ferguson, S.A. Maloy, W.F. Sommer, these Proceedings, p. 66.

[6] M.R. James, S.A. Maloy, W.F. Sommer, P.D. Ferguson, M.M. Fowler, K. Corzine, in: Second International Topical Meeting on Nuclear Applications of Accelerator Technology, Gatlinburg, TN, 20–23 September, 1998, p. 605.

[7] G.J. Willcutt, S.A. Maloy, M.R. James, J. Teague, D.A. Siebe, W.F. Sommer, P.D. Ferguson, in: Second International Topical Meeting on Nuclear Applications of

Accelerator Technology, Gatlinburg, TN, 20–23 September, 1998, p. 254.
[8] M. Ruhle, M. Wilkens, Cryst. Lattice Def. 6 (1975) 129.
[9] S.J. Zinkle, P.J. Maziasz, R.E. Stoller, J. Nucl. Mater. 206 (1993) 266.
[10] N. Yoshida, J. Nucl. Mater. 174 (1990) 220.
[11] N. Hashimoto, E. Wakai, J.P. Robertson, M.L. Grossbeck, A.F. Rowcliffe, Fusion Materials Semiannual Progress Report for Period Ending, 31 December, 1977, DOE/ER-031/23, p. 234.
[12] B.H. Sencer, G.M. Bond, F.A. Garner, S.A. Maloy, W.F. Sommer, M.R. James, in: S.T. Rosinski, M.L. Grossbeck, T.R. Allen, A.S. Kumar (Eds.), Effects of Radiation on Materials, 20th International Symposium, ASTM STP 1405, American Society for Testing and Materials, West Conshohocken, PA, 2002, in press.
[13] G.E. Lucas, J. Nucl. Mater. 206 (1993) 287.
[14] E.H. Lee, J.D. Hunn, T.S. Byun, L.K. Mansur, J. Nucl. Mater. 280 (2000) 18.